On the Kalman Filter Parameter Estimation Methods for Blind Source Separation

Alexandre Miccheleti Lucena, Kenji Nose-Filho, Ricardo Suyama

***Abstract*—Blind Source Separation (BSS) is a well-known problem in signal processing and still receives attention from the scientific community, given its applicability in different areas. This work presents a theoretical background overview of the Kalman Filter formulation and its applicability to the BSS problem as a parameter estimator in two different approaches: joint (JEKF) and dual parameter estimation (DEKF). These approaches are evaluated in different scenarios for first-order autoregressive source signals, with analysis of the initialization details, presenting simulation results and performance comparison with classic algorithms, SOBI and SONS, evaluated by SIR, MER and MSE. The results showed that both the JEKF and DEKF algorithms can perform separation in a two-source-two-mixture scenario. In general, over the scenarios studied, DEKF presented a better performance when compared to the JEKF on the evaluated metrics. However, neither algorithm correctly estimated the parameters for mixtures involving more than two sources, showing convergence issues and sensitivity to initialization for an increased number of sources.**

***Index Terms*—Blind source separation, Kalman filter, parameter estimation, joint estimation, dual estimation, signal processing.**

I. INTRODUCTION

ONE of the many problems faced in signal processing is the Blind Source Separation (BSS), or Blind Signal Separation. This well known problem can be found in applications such as communication systems, geophysics and biomedical signal processing [1]–[3]. It addresses the fact that in certain scenarios the observation of the signals of interest can't be done individually, and even multiple sensors can only perceive a mixture of the sources which are generally simultaneously active. In such cases, there is an interest in applying a procedure over the observed signals to separate or isolate the sources.

An increasing number of works in the last two decades have been exploring the Kalman Filter as a tool for blind source separation. For example, in [4] a expectation-maximization strategy benefits from the Kalman smoother on the E-step. In [5] the algorithm is used to estimate source dynamics for event-related sources. Or as in [6], where it is used for separation in a source tracking task. Most of those works use the Kalman Filter formulation in part of the processing, or introducing extra steps to the formulation to obtain better estimations of the sources of interest. However, it is possible to adapt the Kalman Filter formulation to be applied to BSS more directly.

As to be discussed later, the blind source separation problem formulation can be written as a state-space model in a straightforward way, where the mixing matrix coefficients are considered as unknown parameters of the model. This change in perspective makes the Extended Kalman Filter (EKF) a candidate for the task of estimating both the states and unknown parameters. Although this is a known approach to the problem, the applicability and overall analysis on its performance or limitation are less discussed in the literature and a more in-depth analysis is required.

This formulation particularly benefits from the autoregressive (AR) signal modeling, as an AR signal can be characterized by the poles associated with its time correlation, and easily conveyed to be estimated as an unknown parameter. In this sense, applications that can be modeled as AR process may benefit from this approach. For example, to cite a few, the multispectral image obtained from an airborne visible/infrared imaging spectrometer [7], the speech source separation [8], [9] and financial data analysis [10] help to illustrate scenarios where sources can be modeled as AR processes and are possible candidates for the algorithm application. Yet, an important characteristic of Kalman Filter based algorithms is that the estimation of states (or parameters) are online, meaning that each new sample can be used to update the model and contribute to the estimation, aiding any application that rely on immediate updates.

This work presents a comparison over the two main parameter estimation methods based on the EKF algorithm. These approaches, joint estimation and dual estimation, are submitted to the same conditions and tested for the task of blind source separation of artificially generated AR source signals, where the convergence of the algorithm, initialization strategies and limitations are discussed. For a more in-depth comparison, results of classical algorithms commonly used for similar scenario, such as the Second Order Blind Identification (SOBI) [11] and the Second-Order NonStationary (SONS) [12], are also presented. The performance of each algorithm is evaluated by measuring the signal-to-interference ratio (SIR) between source and estimated signal, where the mixing matrix is evaluated by the Mixing Error Ratio (MER) and parameter estimation by the Mean Squared Error (MSE).

Alexandre Miccheleti Lucena, Kenji Nose-Filho and Ricardo Suyama are with the Engineering, Modeling and Applied Social Sciences Center, Federal University of ABC, Santo André, SP, Brazil (e-mails: {alexandre.lucena, kenji.nose, ricardo.suyama} @ufabc.edu.br) ORCID: 0000-0002-9884-6295, 0000-0002-2559-1973, 0000-0002-8398-5268.

This work was financed in part by the Coordenação de Aperfeiçoamento de Pessoal de Nível Superior - Brasil (CAPES) - Finance Code 001, the National Council for Scientific and Technological Development (CNPq) grant #311380/2021-2, and the São Paulo Research Foundation (FAPESP) grant #2020/09838-0 (BI0S - Brazilian Institute of Data Science).

Submission: 2024-07-26, First decision: 2024-09-17, Acceptance: 2025-03-01, Publication: 2025-03-15.

Digital Object Identifier: 10.14209/jcis.2025.1

II. Problem Definition

The mathematical formulation for the BSS problem considering two sources and two sensors (two mixtures), can be represented as follows:

$$\begin{aligned} z_1(k) &= h_{11}x_1(k) + h_{12}x_2(k)\,, \\ z_2(k) &= h_{21}x_1(k) + h_{22}x_2(k)\,, \end{aligned} \tag{1}$$

where $x_1(k)$ and $x_2(k)$ denote the discrete source signals, and the mixture signals $z_1(k)$ and $z_2(k)$ are obtained by a weighted sum of the sources, given by the weights h_{ij}. In this particular case described by Equation (1), some characteristics as the delay between source and sensors or possible reflections are not present, and it can be classified as a linear, instantaneous and determined (same number of sources and sensors) source separation problem. It is also common to write this linear system by its matrix representation as in

$$\mathbf{z} = \mathbf{H}\mathbf{x} + \mathbf{r}\,, \tag{2}$$

where $\mathbf{z}$ and $\mathbf{x}$ are column vectors containing $z_i(k)$ and $x_i(k)$ respectively, and $\mathbf{H}$ is a matrix containing the coefficients h_{ij}. The vector $\mathbf{r}$ in (2) is an additive noise component, and might be associated with noisy observations, which corrupts the mixture observation. In the BSS context the matrix $\mathbf{H}$ is called the *mixture matrix*, and the goal is to find a transformation over the observed mixtures $\mathbf{z}$ that recover the sources $\mathbf{x}$.

Given a set of observations of mixed signals, and assuming that the mixture matrix $\mathbf{H}$ is invertible, one of the possible solutions can be obtained as finding a separating matrix $\mathbf{W}$ that multiplied by the observations $\mathbf{z}$ is capable of obtaining an estimate $\mathbf{y}$ of the sources. This can be written as:

$$\mathbf{y} = \mathbf{W}\mathbf{z}\,, \tag{3}$$

where in an ideal case the perfect separation would be achieved by finding a $\mathbf{W} = \mathbf{H}^{-1}$ and the estimated source $\mathbf{y}$ would be equal to $\mathbf{x}$. Other approaches to source separation may explore the temporal characteristics of the observations [11], [13], or leverage the sparseness of the sources in the time-frequency domain to estimate a separation mask [14].

III. The Extended Kalman Filter

The *Extended Kalman Filter* (EKF) is an extension of its original formulation which assumes a linearization procedure over the system equations to consider nonlinear systems. The state-space formulation for a nonlinear discrete system may be written as

$$\mathbf{x}_k = f(\mathbf{x}_{k-1}) + \mathbf{w}_{k-1}\,, \tag{4}$$

$$\mathbf{z}_k = h(\mathbf{x}_k) + \mathbf{r}_k\,, \tag{5}$$

$$p(\mathbf{w}_k) \sim \mathcal{N}(0,\, \mathbf{Q})\,, \tag{6}$$

$$p(\mathbf{v}_k) \sim \mathcal{N}(0,\, \mathbf{R})\,, \tag{7}$$

being (4) and (5) the state and observation equations respectively. The state equation represents how the state vector $\mathbf{x}$ will change at each iteration k (subscript). The current state $\mathbf{x}_k$ is a composition of the previous state $\mathbf{x}_{k-1}$ transformed by a function $f(.)$ that is obtained by the model of study and its relation with the state vector. The $\mathbf{w}_{k-1}$ vector models the possible influence of noise over the state process, and is assumed to have a normal distribution with zero mean and variance $\mathbf{Q}$. There are cases where the current state cannot be observed directly, and the observation output $\mathbf{z}_k$ is a function of the state, meaning there might be some underlying dynamics to be considered on the measurements, that can be represented by a function $h(.)$. In this equation, $\mathbf{r}_k$ represent the observation noise. Here, $\mathbf{r}_k$ is also assumed to have a normal distribution with zero mean and variance $\mathbf{R}$.

For this kind of system, the state transition and state observation are determined by a nonlinear function, that need to be linearized for the application of the Kalman Filter formulation. The linearization is obtained through a Taylor series expansion over the state equation and measurement equation, where the transition matrix and observation matrices can be determined by the following partial derivatives

$$\mathbf{F}_k = \left.\frac{\partial f_k}{\partial \mathbf{x}}\right|_{\hat{\mathbf{x}}_k}\,, \tag{8}$$

$$\mathbf{H}_k = \left.\frac{\partial h_k}{\partial \mathbf{x}}\right|_{\hat{\mathbf{x}}_k^-} \tag{9}$$

and $\mathbf{F}_k$ and $\mathbf{H}_k$ are often called the *transition* and *observation* matrices, respectively. After the proper linearization procedure, with the partial derivatives matrices, the equations for the EKF algorithm remains the same as the linear Kalman Filter. The state estimation for the EKF is given by the following algorithm (Algorithm 1).

Algorithm 1 Extended Kalman Filter (EKF)

Initialization

$$\begin{aligned} \hat{\mathbf{x}}_0 &= E[\mathbf{x_0}] \\ \mathbf{P}_0 &= E[(\mathbf{x}_0 - \hat{\mathbf{x}}_0)(\mathbf{x}_0 - \hat{\mathbf{x}}_0)^T] \end{aligned}$$

Prediction

$$\begin{aligned} \hat{\mathbf{x}}_k^- &= \mathbf{F}_{k-1}\hat{\mathbf{x}}_{k-1} \\ \mathbf{P}_k^- &= \mathbf{F}_{k-1}\mathbf{P}_{k-1}\mathbf{F}_{k-1}^T + \mathbf{Q} \end{aligned}$$

Update

$$\begin{aligned} \mathbf{K}_k &= \mathbf{P}_k^-\mathbf{H}_k^T(\mathbf{H}_k\mathbf{P}_k^-\mathbf{H}_k^T + \mathbf{R})^{-1} \\ \hat{\mathbf{x}}_k &= \hat{\mathbf{x}}_k^- + \mathbf{K}_k(\mathbf{z}_k - \mathbf{H}_k\hat{\mathbf{x}}_\mathbf{k}^-) \\ \mathbf{P}_k &= (\mathbf{I} - \mathbf{K}_k\mathbf{H}_k)\mathbf{P}_k^- \end{aligned}$$

IV. Source Separation and Parameter Estimation

The modeling of the BSS problem as a state-space system might be straightforward if we compare both formulations, specially Equations (2) and (5) (the notation was chosen carefully to highlight the similarities); it is possible to treat the mixtures as *observation* of the sources (states) mixed by some observation (mixture) matrix. Usually for the BSS problem the kind of mixing process over the source signals is assumed (linear, convolutive, non-linear, etc.), and can be used for defining the transition matrix structure and state dynamic, but the observation/mixing matrix is generally treated as unknown (blind).

For the parameter estimation, one alternative is to associate the unknown terms of the mixing matrix as the parameters to be estimated, and since $\mathbf{H}_k$ is assumed to be constant we may drop the subscript k in (10), so each element of the matrix $\mathbf{H}$ is treated as an unknown constant parameter. If the sources are modeled, for example, by an AR(p) model, one may be interested in estimating the source dynamics and transition matrix $\mathbf{F}_k$ so its elements can be associated with unknown parameters. In this case, also considering that the AR coefficients are constant and dropping the subscript k, we may represent the transition matrix as

$$\mathbf{F} = \begin{bmatrix} p_1 & 0 & \cdots & 0 \\ 0 & p_2 & \ddots & \vdots \\ \vdots & \ddots & \ddots & 0 \\ 0 & \cdots & 0 & p_N \end{bmatrix}, \mathbf{H} = \begin{bmatrix} \theta_{11} & \cdots & \theta_{1j} \\ \vdots & \ddots & \vdots \\ \theta_{i1} & \cdots & \theta_{ij} \end{bmatrix} \tag{10}$$

where the main diagonal contains the AR(p) coefficients (or poles) p_i ($i = 1, ..., N$) for the N sources, and may also be treated as unknown parameters. Considering that the sources are uncorrelated, the off-diagonal values in $\mathbf{F}$ are zero. In this case not only the sources $\mathbf{x}_k$ need to be estimated but also the matrix $\mathbf{H}_k$, characterizing it as a simultaneous state and parameter estimation problem, which the EKF formulation is able to handle after some proper modifications to be discussed in the following sections.

A. A modeling example

To illustrate the described modeling of the BSS problem, the following state-space equations are presented as an example. This may represent the *true* model that underlies the BSS problem as a state-space equation, without any concern about the parameter estimation task yet. The following example considers two sources ($N = 2$), generated by an AR(1) model, and two mixtures ($M = 2$). In this case, the state equation that describes the dynamics of the source is

$$\begin{bmatrix} x_1 \\ x_2 \end{bmatrix}_k = \begin{bmatrix} p_1 & 0 \\ 0 & p_2 \end{bmatrix} \begin{bmatrix} x_1 \\ x_2 \end{bmatrix}_{k-1} + \begin{bmatrix} w_1 \\ w_2 \end{bmatrix}_k, \tag{11}$$

and for the measurement equation, we can write

$$\begin{bmatrix} z_1 \\ z_2 \end{bmatrix}_k = \begin{bmatrix} \theta_{11} & \theta_{12} \\ \theta_{21} & \theta_{22} \end{bmatrix} \begin{bmatrix} x_1 \\ x_2 \end{bmatrix}_k + \begin{bmatrix} r_1 \\ r_2 \end{bmatrix}_k. \tag{12}$$

From equations (11) and (12), it is possible to highlight that the parameters of interest to be estimated are associated with the matrices $\mathbf{F}$ and $\mathbf{H}$. The reformulation of the state-space equation may be needed according to the parameters estimation algorithm to be used (joint or dual), but the main idea regarding the relation between BSS and the parameter estimation is defined. The purpose of this simple example is just to enlighten the idea of the BSS problem as a state-space formulation and which are the parameters to be estimated in the model. In the following sections, the specific application of the JEKF and DEKF using this model is conducted.

B. State and parameter joint estimation

One of the earliest works to propose a joint estimation approach is [15], and it suggests unknown parameters to be included into the state vector directly, so state and unknown parameters are estimated *jointly*. This is achieved by associating the unknown parameters θ of the system to the state vector, and creating an augmented state vector as in

$$\begin{bmatrix} \mathbf{x}_k \\ \theta_k \end{bmatrix} = \begin{bmatrix} f(\mathbf{x}_{k-1}, \theta_{k-1}) + \mathbf{w}_{k-1} \\ \theta_{k-1} + \mathbf{v}_{k-1} \end{bmatrix}, \tag{13}$$

$$\mathbf{z}_k = h(\mathbf{x}_k, \theta_k) + \mathbf{r}_k \ . \tag{14}$$

This joint estimation of state and parameters (JEKF) approach for source separation EKF is explored in [16]. By modeling the sources as AR signals, the mixture matrix coefficients (unknown parameters) are estimated by creating an augmented vector as in (13) and following the state estimation procedure for the augmented vector with the EKF formulation. In said work, the AR coefficients of the sources are considered exactly known, and the only unknown parameters are the mixture matrix coefficients to be estimated.

The application of the EKF formulation in the above system equations is straightforward, but in this case, although the $\mathbf{F}_k$ and $\mathbf{H}_k$ matrices (8) and (9) are obtained through the same linearization step respectively, now both depend on the augmented state vector, and function $h(.)$ in (14) also depends on the unknown parameters.

C. State and parameter dual estimation

An alternative from creating an augmented vector is to estimate states and parameters separately (yet simultaneously) with an independent EKF formulation for each [17]. The EKF formulation can be used to implement a dedicated EKF for the state estimation, and another EKF for the parameter estimation, hence the name Dual Kalman Filter (DEKF) [18]. The main idea behind the DEKF is the combination of two EKF running in parallel, one implementing its classic state estimation procedure, assuming known system parameters, and the second EKF running simultaneously, having the parameters to be estimated as state vectors of the system by considering the state estimates to be known. One of the earliest approaches into using the DEKF as a signal separation tool was found in [19], where the DEKF is used to train the weights of a couple parallel neural network that separates two speech sources in a monoaural signal.

There are also specific approaches using the DEKF as a parameter estimation tool in BSS context. The works [20], [21], and [22] utilizes the DEKF formulation by modeling the source dynamic and mixture matrix estimation as parameters to be estimated. Differently from the joint estimation approach, in the dual estimation the augmented vector is separated to be estimated in parallel. The first EKF, dedicated to state estimation, follows the traditional estimation steps of the algorithm as in (4), however the state dynamics should now incorporate the unknown parameters θ as

$$\mathbf{x}_k = f(\mathbf{x}_{k-1}, \theta) + \mathbf{w}_k \ , \tag{15}$$

$$\mathbf{z}_k = h(\mathbf{x}_k, \theta) + \mathbf{r}_k \ . \tag{16}$$

On the other hand, there is a parallel EKF formulation dedicated to estimate the parameters that will follow the traditional EKF algorithm, but the state vector of this filter are the unknown parameters organized in a parameter vector. The dynamic of its observation should be written in function of the actual process state, that are considered as known. The state-space equations for the parameter estimation EKF are described as

$$\theta_k = \theta_{k-1} + \mathbf{v}_{k-1}\,, \tag{17}$$
$$\mathbf{z}_k = g(\mathbf{x}_k, \theta_k) + \mathbf{m}_k\,, \tag{18}$$
$$p(\mathbf{v}_k) \sim \mathcal{N}(0,\, \mathbf{Q}^{\theta})\,, \tag{19}$$
$$p(\mathbf{m}_k) \sim \mathcal{N}(0,\, \mathbf{R}^{\theta})\,. \tag{20}$$

The state vector will contain the source estimations, whilst the parameter vector may contain matrices $\mathbf{F}_k$ and $\mathbf{H}_k$ coefficients. Since there are two EKF equations in the algorithm, variables that are repeated in each filter will have a superscript needed to distinguish them between the state and estimation filter $\mathbf{x}$ and the parameter estimation filter θ. The DEKF algorithm can be summarized by the following equations (Algorithm 2).

Algorithm 2 Dual Extended Kalman Filter (DEKF)

INITIALIZATION

$$\hat{\mathbf{x}}_0 = E[\mathbf{x_0}]$$
$$\hat{\theta}_0 = E[\theta_{\mathbf{0}}]$$
$$\mathbf{P}_0^{\mathbf{x}} = E[(\mathbf{x}_0 - \hat{\mathbf{x}}_0)(\mathbf{x}_0 - \hat{\mathbf{x}}_0)^T]$$
$$\mathbf{P}_0^{\theta} = E[(\theta_0 - \hat{\theta}_0)(\theta_0 - \hat{\theta}_0)^T]$$

PARAMETER FILTER PREDICTION

$$\hat{\theta}_k^- = \hat{\theta}_{k-1} \;\; \mathbf{P}_k^{\theta-} = \mathbf{P}_{k-1}^{\theta} + \mathbf{Q}^{\theta}$$

STATE FILTER PREDICTION

$$\hat{\mathbf{x}}_k^- = \mathbf{F}_{k-1}\hat{\mathbf{x}}_{k-1}$$
$$\mathbf{P}_k^{\mathbf{x}-} = \mathbf{F}_{k-1}\mathbf{P}_{k-1}^{\mathbf{x}}\mathbf{F}_{k-1}^T + \mathbf{Q}^{\mathbf{x}}$$

STATE FILTER UPDATE

$$\mathbf{K}_k^{\mathbf{x}} = \mathbf{P}_k^{\mathbf{x}-}\mathbf{H}_k^T(\mathbf{H}_k\mathbf{P}_k^{\mathbf{x}-}\mathbf{H}_k^T + \mathbf{R}^{\mathbf{x}})^{-1}$$
$$\hat{\mathbf{x}}_k = \hat{\mathbf{x}}_k^- + \mathbf{K}_k^{\mathbf{x}}(\mathbf{z}_k - \mathbf{H}_k\hat{\mathbf{x}}_{\mathbf{k}}^-)$$
$$\mathbf{P}_k^{\mathbf{x}} = (\mathbf{I} - \mathbf{K}_k^{\mathbf{x}}\mathbf{H}_k)\mathbf{P}_k^{\mathbf{x}-}$$

PARAMETER FILTER UPDATE

$$\mathbf{K}_k^{\theta} = \mathbf{P}_k^{\theta-}\mathbf{G}_k^T(\mathbf{G}_k\mathbf{P}_k^{\theta-}\mathbf{G}_k^T + \mathbf{R}^{\theta})^{-1}$$
$$\hat{\theta}_k = \hat{\theta}_k^- + \mathbf{K}_k^{\theta}(\mathbf{z}_k - \mathbf{H}_k\hat{\mathbf{x}}_{\mathbf{k}}^-)$$

The EKF for parameter estimation must consider that the dynamics between the states and the unknown parameters follows a certain known (assumed) model, and the linearization of this dynamic is represented by the matrix $\mathbf{G}_k$ as

$$\mathbf{G}_k = \mathbf{H}_k \frac{\partial \hat{\mathbf{x}}_k^-}{\partial \theta}\bigg|_{\theta=\hat{\theta}_k^-}\,. \tag{21}$$

TABLE I
INITIALIZATION VALUES FOR THE $\mathbf{Q}$, $\mathbf{R}$ AND $\mathbf{P}$ MATRICES IN THE JEKF AND DEKF ALGORITHMS - $\mathbf{I}$ IS THE IDENTITY MATRIX.

	$\mathbf{Q}_0^{\mathbf{x}}$	$\mathbf{Q}_0^{\boldsymbol{\theta}}$	$\mathbf{R}_0^{\mathbf{x}}$	$\mathbf{R}_0^{\boldsymbol{\theta}}$	$\mathbf{P}_0^{\mathbf{x}}$	$\mathbf{P}_0^{\boldsymbol{\theta}}$
JEKF	$9 \times 10^{-2}\,\mathbf{I}$	$10^{-6}\,\mathbf{I}$	$\mathbf{I}$	-	$10^{-3}\,\mathbf{I}$	$10^{-3}\,\mathbf{I}$
DEKF	$10^{5}\,\mathbf{I}$	$10^{-6}\,\mathbf{I}$	$\mathbf{I}$	$\mathbf{I}$	$10^{-3}\,\mathbf{I}$	$10^{-3}\,\mathbf{I}$

V. EXPERIMENTAL SETUP

A. Algorithm Initialization

There are two groups of parameters associated with the JEKF and DEKF algorithms that need to be initialized before the algorithm's first iteration: the unknown states and parameters, and the covariance matrices associated with noise and error. Except when stated otherwise, the simulation results in this section were obtained according to the following described initialization procedure.

For the unknown states associated with the source estimation, the $\mathbf{x}_0$ values were initialized with zeros. For the AR coefficients, the chosen procedure was a random initialization, obtained from an independent random uniform distribution between -0.3 and 0.3.

As the main task is to deal with the BSS problem, where the mixing (observation) matrix $\mathbf{H}_0$ is not known, so the initialization of this matrix greatly affects the algorithm progression, since it relates to the observation of the states. At first, there were attempts on initializing the mixing matrix randomly. However, this method did not show consistency. Assuming that in each observed mixture there is only one (exclusive/unique) predominant source signal that is not predominant in other mixtures (e.g. mixture one is predominantly composed by source one, and mixture two by source two, and so on...), another approach was to initialize the mixing matrix as an identity matrix $\mathbf{I}$. This method showed more reliability since the mixtures presented the condition required.

Given the lack of knowledge about a proper initialization procedure for the covariance matrices, in the following proposed base example, the matrices $\mathbf{Q}$, $\mathbf{R}$ and $\mathbf{P}$ in each algorithm were manually tuned to achieve separation and be established as the initial conditions for the experiments. Each matrix is obtained by generating an identity matrix $\mathbf{I}$ with the matching dimension associated with the number of states or parameters, and then multiplied by a scaling factor. Tab. I summarizes the initialization value for each parameter and algorithm.

B. Performance Comparison

As a quantitative performance comparison, the quality of the recovered source signals was calculated by the SIR. In summary, the SIR evaluates the ratio between the energy of the target source x_j and the energy of the residual interference signal (i.e. difference between estimated and true signal) $e_j[k] = \hat{x}_j[k] - x_j[k]$ as in

$$\text{SIR}_j := 10\log_{10}\frac{\sum_k x_j^2[k]}{\sum_k e_j^2[k]}\,. \tag{22}$$

There is also an interest in evaluating the estimated mixing matrix. Each column of the mixing matrix $\mathbf{H}$ contains the weights h_{ij} associated to a given source j, and those coefficients can be grouped as a vector $\mathbf{h}_j$. Through least-squares projection, the estimated vector of mixing coefficients $\widehat{\mathbf{h}}_j$ is decomposed in a collinear $\mathbf{h}_j^{\text{coll}}$ and orthogonal $\mathbf{h}_j^{\text{orth}}$ to the true vector of mixing coefficients $\mathbf{h}_j$, in a way that

$$\widehat{\mathbf{h}}_j = \mathbf{h}_j^{\text{coll}} + \mathbf{h}_j^{\text{orth}}. \tag{23}$$

The Mixing Error Ratio (MER) [23] calculates the quality of the matrix coefficients or mixing gains for each source in comparison to the original mixing matrix, allowing arbitrary scaling of the matrix coefficients for each source. The MER in decibels is obtained by

$$\text{MER}_j = 10\log_{10}\frac{\left\|\mathbf{h}_j^{\text{coll}}\right\|^2}{\left\|\mathbf{h}_j^{\text{orth}}\right\|^2}\ . \tag{24}$$

VI. Simulation Results

The JEKF and DEKF algorithms were implemented in a simulation environment following the initialization procedure described in Section V-A. Although the aim of this paper is to explore the JEKF and DEKF algorithm behavior and performance, there are other algorithms that are known for their effectiveness in the considered scenario. One example is the SOBI [11] algorithm, that leverages the second-order statistics of the signals and are commonly applied when the sources present time correlation, which is the case for AR signals. An extension of the SOBI algorithm is the SONS [12] algorithm that improves SOBI by also utilizing any second-order nonstationarity present within the sources, yet the data in the simulations are considered as stationary. All four algorithms are tested on the same scenario in order to compare the JEKF and DEKF approaches with more classical algorithms (SOBI and SONS) as baseline results.

One important difference to consider is that SOBI and SONS are batch algorithms (i.e. need all the data to be processed for a proper estimation of the mixing matrix), while both JEKF and DEKF are online algorithms (i.e. can update de estimated mixing matrix after each iteration). As a way to compensate this difference, at the last iteration of JEKF and DEKF algorithms, the final estimated mixing matrix was inverted and used to separate the mixed signals. This generates an estimate of the sources as in (3) for SIR and MER evaluation, hence comparing all the algorithms as batch algorithms. The online estimation capabilities of the parameters were analyzed in terms of MSE, where SOBI and SONS are not considered as they do not present online parameter estimates.

Simulation results are organized as follows. Section VI-A explore the algorithms considering different pole values for the sources and diffrent mixing matrices on the separation of two sources (and observations) in a way that a more general behavior and understanding of the JEKf and DEKF algorithms is obtained. Section VI-B consider the results observed in VI-A for the analysis of JEKF and DEKF algorithms on favorable conditions and analyze their online parameter estimation capabilities. Section VI-C propose a study of the JEKF and DEKF algorithms performance when the number of sources is increased.

A. Source AR pole and mixing conditions

A simple case to be considered in a source separation problem is the separation of two signals, as described in Section IV, hence this experimental setup is an investigation of the JEKF and DEKF algorithms behavior on the separation of two sources (and observations), inspired by the conditions presented in [16]. Considering that the sources are modeled as AR signals, the time correlation and spectra of the signal are directly associated to the pole values used to generate the sources. Synthetic sources were generated from independent white random Gaussian distributions and modeled as first-order AR(1) sources, each one with 5000 samples. With that in mind, different pole values were tested for the generation of the source signals varying from -0.95 to 0.95 (with steps of 0.05) for each source, leading to a combination of each possible pole value p_i between source 1 and 2.

To test this scenario, a mixing matrix was chosen arbitrarily to simulate the observed signals, mixing the source signals as the operation described in Equation (2) with the following matrix

$$\mathbf{H} = \begin{bmatrix} 0.8575 & 0.5145 \\ 0.3511 & 0.9363 \end{bmatrix}, \tag{25}$$

where each row of the matrix has a unitary norm. The obtained mixed signals where separated using JEKF, DEKF, SOBI and SONS algorithms and the SIR calculated over each recovered source. To better summarize the results on a unique SIR value and later be able to plot a single 3D surface, the SIR obtained for sources 1 and 2 were summed and divided by two (averaged). The said experiment was repeated 50 times (Monte Carlo), maintaining the same AR poles variation, mixing matrix, and rules for initialization, so every variable that depended on random sampling, such as parameters initialization and the AR signal exciting noise were resampled. Fig. 1 show the results of the mean SIR calculated over the recovered signals for the 50 realizations, considering each combination of pole value between the proposed interval (-0.95 to 0.95).

From Fig. 1, one can observe a general behavior of the separation algorithms for different poles of the AR(1) sources. It is possible to observe that for all algorithms there is a decrease in performance when $p_1 = p_2$ as the signals start to present similar time correlation (or spectral content), and might be indistinguishable from each other. However as pole values start do differ, each algorithm have their own characteristics. The JEKF seem to perform poorly when compared to other algorithms, peaking its SIR values around 40 dB, close to the point where both poles are closer to 1 (above 0.8) but with opposite sign ($p_1 = -p_2$). For the DEKF, a similar behavior is observed, however the overall performance is increased in a much wider area (above 0.5) peaking closer to 60 dB near $p_1 = -p_2 = 0.9$ and diminishing elsewhere. SOBI and SONS have a smoother surface, meaning they present a more balanced performance across the tested values, with SOBI closer to 50 dB and SONS slightly below, near 45 dB. However, although it is not a global behavior across all values,

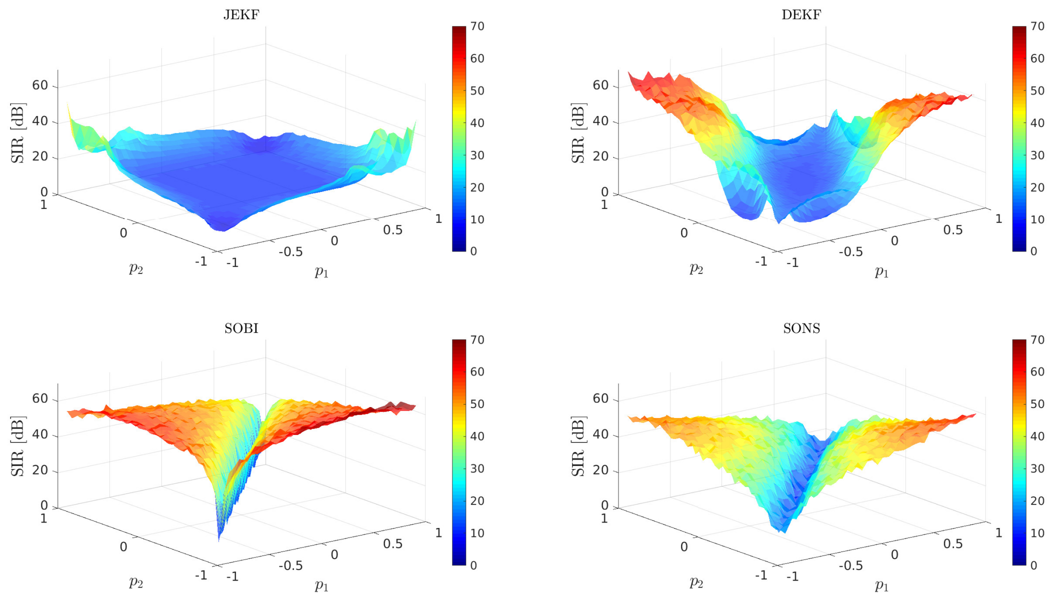

Fig. 1. Mean SIR values in decibels of the recovered sources for different pole values p_i over 50 simulations of the JEKF (top-lef), DEKF (top-right), SOBI (bottom-left) and SONS (bottom-right) algorithms in a two-source-two-mixture scenario (N = M = 2).

it is important to notice that the peak mean values stand for the DEKF in the analyzed scenario, specially when $p_1 = -p_2 > 0.6$ where the DEKF not only match SOBI performance but surpasses it as it get closer to 1.

Another important aspect of the algorithms evaluation is that the chosen mixing matrix can greatly impact on the algorithms performance. To address this fact, the algorithms were tested using a random mixing matrix and had the results evaluated trough SIR and MER. The mixing matrix coefficients were sampled from an uniform distribution between -1 and 1, and then followed by row normalization. In this scenario, two pair of pole values were chosen from the previous simulation to represent a more favorable and unfavorable scenario for the algorithm, as the only parameter being varied are the mixing matrices and sources exciting noise.

Tab. II presents the results of Mean SIR and MER values obtained in 100 simulations for random mixing matrices and sources generated with $p_1 = -p_2 = 0.9$, being considered as a favorable scenario for all the considered algorithms. Results show that JEKF and DEKF algorithms are able to improve the source estimations, with a great advantage for the DEKF algorithm. It is noticeable that the SIR and MER values for the JEKF and DEKF presented more fluctuation, as observed in the greater standard deviation values when compared to SOBI and SONS, that had more consistent results. This indicates that even for a favorable sources, the JEKF and DEKF algorithms are both sensitive on mixing matrix variation, when compared to SOBI and SONS.

Similarly, Tab. III presents the results of Mean SIR and MER values obtained in 100 simulations for random mixing matrices and sources generated with $p_1 = -p_2 = 0.3$, considered as an unfavorable scenario based on Fig. 1. In this scenario, all algorithms have a significant decrease in performance. The JEKF algorithm is the most affected since its mean results are comparable to the observed signals itself, indicating it was not able to recover the sources. As expected from previous discussion, as the source pole values are $p_1 = -p_2 < 0.6$, results show the inability of the DEKF on recovering the sources and also mixing matrix sensitivity as the SIR and MER standard deviation are relatively high. Although the performance decreased, SOBI and SONS maintained consistent results for the random mixing matrix scenario.

Summarily, the SIR surface evaluation and mixing matrix variations show that the SOBI and SONS algorithms are more

TABLE II
MEAN SIR AND MER (AND STANDARD DEVIATION) VALUES OBTAINED FOR RANDOM MIXING MATRICES IN 100 SIMULATIONS FOR N = M = 2 ON A FAVORABLE SCENARIO $p_1 = -p_2 = 0.9$.

	SIR [dB]		MER [dB]	
	Source 1	Source 2	Source 1	Source 2
Mixed	8.6 ± 8.3	9.9 ± 9.0	-	-
JEKF	23.9 ± 12.6	28.3 ± 13.8	30.6 ± 12.7	26.8 ± 12.0
DEKF	**31.4** ± 15.3	30.5 ± 16.9	31.3 ± 21.9	33.2 ± 19.9
SOBI	29.3 ± 8.9	**49.3** ± 6.2	**58.6** ± 13.1	**57.0** ± 9.0
SONS	28.6 ± 7.9	43.4 ± 5.5	45.6 ± 9.6	48.8 ± 13.8

TABLE III
MEAN SIR AND MER (AND STANDARD DEVIATION) VALUES OBTAINED FOR RANDOM MIXING MATRICES IN 100 SIMULATIONS FOR N = M = 2 ON A UNFAVORABLE SCENARIO $p_1 = -p_2 = 0.3$.

	SIR [dB]		MER [dB]	
	Source 1	Source 2	Source 1	Source 2
Mixed	8.6 ± 8.2	9.8 ± 9.0	-	-
JEKF	8.7 ± 8.3	10.0 ± 9.6	7.9 ± 8.8	6.8 ± 7.9
DEKF	15.6 ± 11.1	17.1 ± 12.4	17.2 ± 12.1	16.0 ± 11.8
SOBI	**34.6** ± 5.9	**37.3** ± 5.8	**44.0** ± 11.2	**46.6** ± 13.7
SONS	27.9 ± 6.6	29.5 ± 7.7	33.8 ± 13.5	34.5 ± 11.0

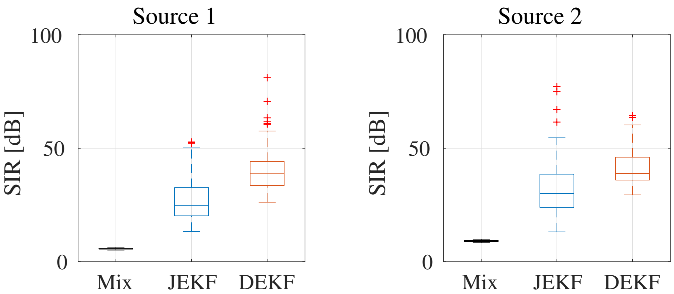

Fig. 2. SIR values for 100 simulations of the DEKF and JEKF algorithm for N = M = 2.

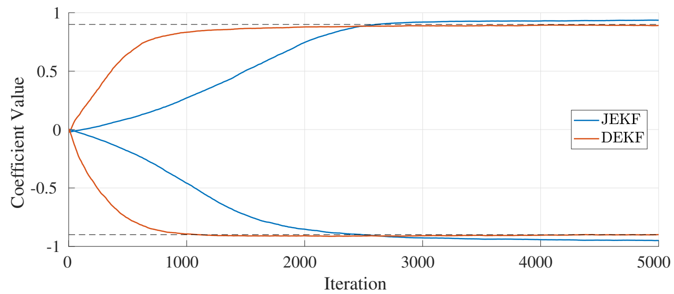

Fig. 3. Evolution of the mean value for the estimated AR parameters in 100 simulations of the DEKF and JEKF algorithm for N = M = 2.

suitable for the batch source separation task, yet the main advantage of using an online algorithm as the Kalman Filter is not explored on this scenario, since the SOBI and SONS are batch algorithms and the adaptive behavior of the EKF algorithm is set aside. Next section address this matter by evaluatig the parameter estimation capabilities of JEKF and DEKF algorithms using MSE.

B. Two Sources

Considering the results obtained in VI-A, a general favorable scenario was established for other aspects of the DEKF and JEKF algorithms could be explored. Two aspects greatly differ from the compared algorithms: the parameter estimation approach and the online estimation capability. In this sense, the following simulations were designed considering fixed source poles $p_1 = -p_2 = 0.9$ and the arbitrarily chosen mixing matrix (25).

To summarize the statistics obtained for the different metrics, the results of SIR are presented in Fig. 2 as a boxplot based on 100 realizations of the experiment. As the poles and mixing matrices are fixed, it implies that the only difference between realizations are random initializations and exiting noise for the sources. Results for the mixed signals (Mix) were also calculated as a way to compare the improvement obtained by the separation.

The SIR median obtained through the simulations for the JEKF for sources one and two were 37.8 dB and 37.5 dB respectively, while the DEKF presented some advantages with median values of 42.5 dB and 43.9 dB. Both algorithms performed similarly for the MER; JEKF obtained 36.5 dB and 41.1 dB medians for sources one and two, respectively, while the DEKF resulted in 42.0 and 43.5.

From Fig. 3 and Fig. 4 it is possible to evaluate the overall behavior of the estimated parameters. Fig. 3 shows the evolution of the mean value for the estimated AR poles while Fig. 4 shows mixing matrix coefficients MSE. As both algorithms iterate, it is possible to observe the convergence of both the estimated poles and mixing matrix coefficients, with a faster response for the DEKF algorithm. The convergence to the true parameter indicates the capacity of tracking the possible underlying parameter that define the model, and could be expected even if the data does not exactly match the AR model. Tab. IV summarizes the results of mean SIR and MER for all algorithms in the proposed scenario, maintaining

TABLE IV
MEAN SIR AND MER VALUES OF THE RECOVERED SIGNALS FOR THE JEKF, DEKF, SOBI AND SONS ALGORITHMS FROM 100 SIMULATIONS FOR A FIXED MIXING MATRIX AND $p_1 = -p_2 = 0.9$ (N = M = 2).

	SIR [dB]		MER [dB]	
	Source 1	Source 2	Source 1	Source 2
Mixed	5.7 ± 0.3	9.1 ± 0.3	-	-
JEKF	27.3 ± 9.3	32.4 ± 12.0	35.3 ± 11.8	32.4 ± 9.4
DEKF	**40.4** ± 9.5	41.4 ± 8.3	44.2 ± 8.3	45.6 ± 9.6
SOBI	29.3 ± 8.9	**49.3** ± 6.2	**58.4** ± 11.4	**58.6** ± 7.4
SONS	28.6 ± 7.9	43.4 ± 5.5	44.8 ± 9.3	44.9 ± 11.8

SOBI and SONS as baseline comparison algorithms, where the DEKF matches SONS results but SOBI still offers better overall results. However, it is important to note that JEKF and DEKF are being trained online (without the knowledge of all training samples in all iterations), as illustrated by Fig. 3 and Fig. 4, and the SOBI and SONS are being trained offline.

C. Three Sources

The source separation problem is not limited to estimating only two sources and ideally an algorithm should be able to handle different numbers of sources and mixtures. The model presented in Section IV is applicable to any number of sources, along with the JEKF and DEKF algorithms. Based on this principle, simulations were conducted using both algorithms in a similar scenario, but with three mixtures of three sources. Fig. 5 and Fig. 6 display the mean value over 100 simulations for the evolution of the AR parameters and MSE of the mixing matrix coefficients, respectively, in the N = M = 3 scenario. Although the implementation of both algorithms may be straightforward for an increased number of sources, Fig. 5 and Fig. 6 demonstrate that their behavior over the estimated parameters in the simulated scenario changes dramatically.

Fig. 5 show that for the JEKF algorithm, none of the poles converged to their true value, and although the mixing matrix parameters estimation seems stable, it did not reflected in a good source estimation (SIR). For the DEKF, one of the sources (AR coefficient of -0.9) the estimation was successful, however, the other two coefficient estimation seems to collapse as both parameters converge to the same value of approximately 0.75.

In Fig. 6, its possible to observe for the DEKF that there are two coefficients which, besides initialized relatively close to their true values, diverged from the expected value; at the same interval (around iteration 1000 and 2000) one coefficient from

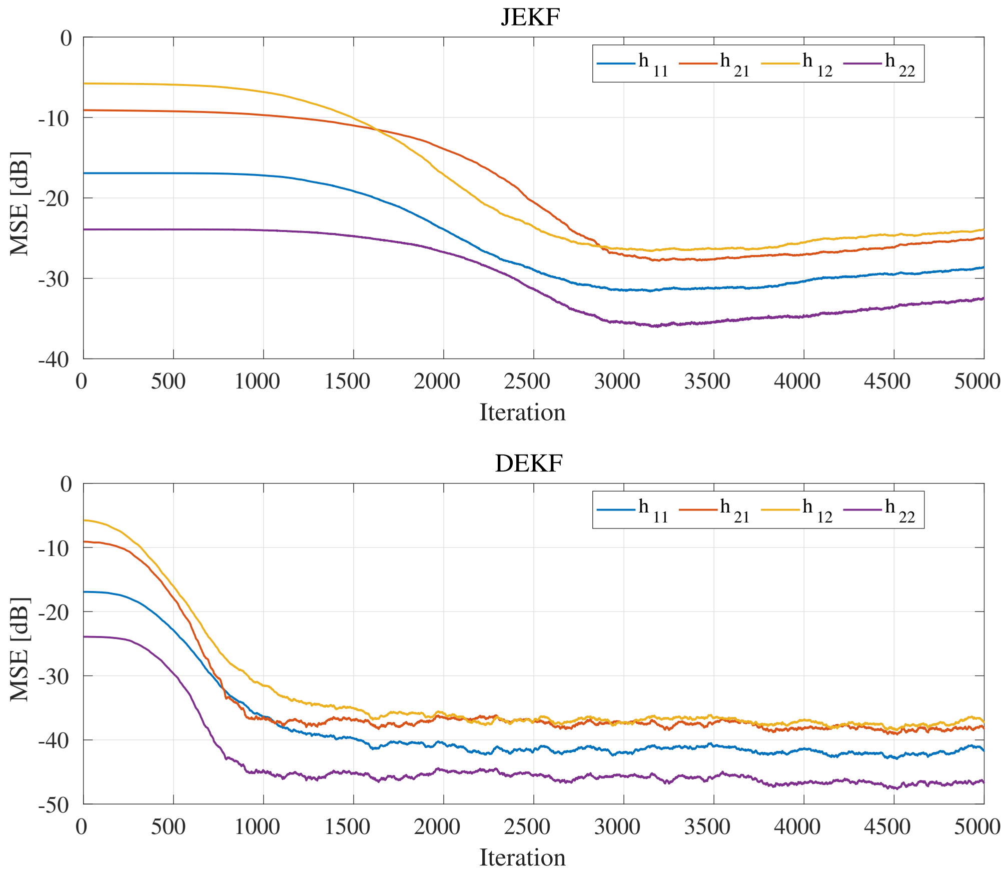

Fig. 4. Mean squared error for the estimated mixing matrix coefficients in 100 simulations of the DEKF (bottom) and JEKF (top) algorithm for N = M = 2.

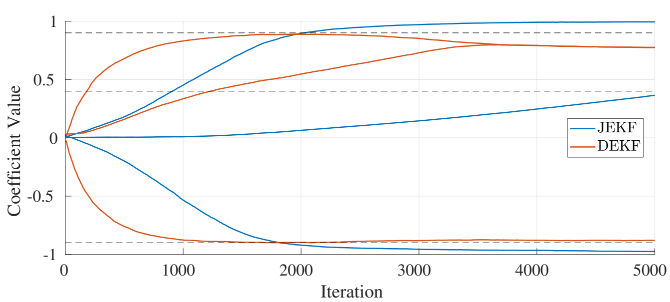

Fig. 5. Evolution of the mean value for the estimated AR parameters in 100 simulations of the DEKF and JEKF algorithm for N = M = 3.

the main diagonal (h_{11}) decreases, while an off-diagonal value increases (h_{12}). This indicates that the algorithm is discarding the estimation for one of the sources, to estimate a duplicate signal, as two poles (Fig. 5 and two rows of the estimated mixing matrix (Fig. 6) are converging to similar values.

Evaluating the sources estimation quality, Fig. 7 presents the SIR values obtained in the 100 repetitions for the $N = M = 3$ scenario. From the SIR values, its possible to determine that the quality of the source estimation was definitely poorer when compared to the $N = M = 2$ scenario. The SIR median obtained by the simulations in this experiments for JEKF for sources one two, and three was 12.8 dB, 15.8 dB and 17.0 dB respectively, while the DEKF presented median values of 2.9 dB, 3.2 dB and 16.0 dB. Tab. V summarizes the results of mean SIR for all the considered algorithms on the $N = M = 3$ scenario, where results for SOBI and SONS are also present. Results from the mean SIR confirm that both DEKF and JEKF were unable to retrieve the sources, while SOBI and SONS, beside the fact that de SIR also decreased when compared with two sources scenario, presented relatively good performance.

TABLE V
MEAN SIR VALUES OF THE RECOVERED SIGNALS FOR THE JEKF, DEKF, SOBI AND SONS ALGORITHMS FROM 100 SIMULATIONS FOR A FIXED MIXING MATRIX, $p_1 = -p_3 = 0.9$ AND $p_2 = 0.4$ (N = M = 3).

	SIR [dB]		
	Source 1	Source 2	Source 3
Mixed	9.5 ± 0.3	2.4 ± 0.1	15.4 ± 0.3
JEKF	12.8 ± 0.4	15.8 ± 1.8	17.0 ± 0.6
DEKF	2.9 ± 0.6	3.2 ± 0.2	16.6 ± 9.3
SOBI	**28.9** ± 7.6	**31.3** ± 4.4	**44.8** ± 3.6
SONS	21.9 ± 5.4	23.0 ± 5.4	34.9 ± 6.8

VII. Conclusion

This work presented two algorithms for blind source separation (BSS) using the Kalman Filter formulation based on parameter estimation approach. The Kalman filter formulation enables the development of an online algorithm, an important characteristic for several applications. The theoretical background of the algorithms was described, along with their applications in BSS and performance comparison.

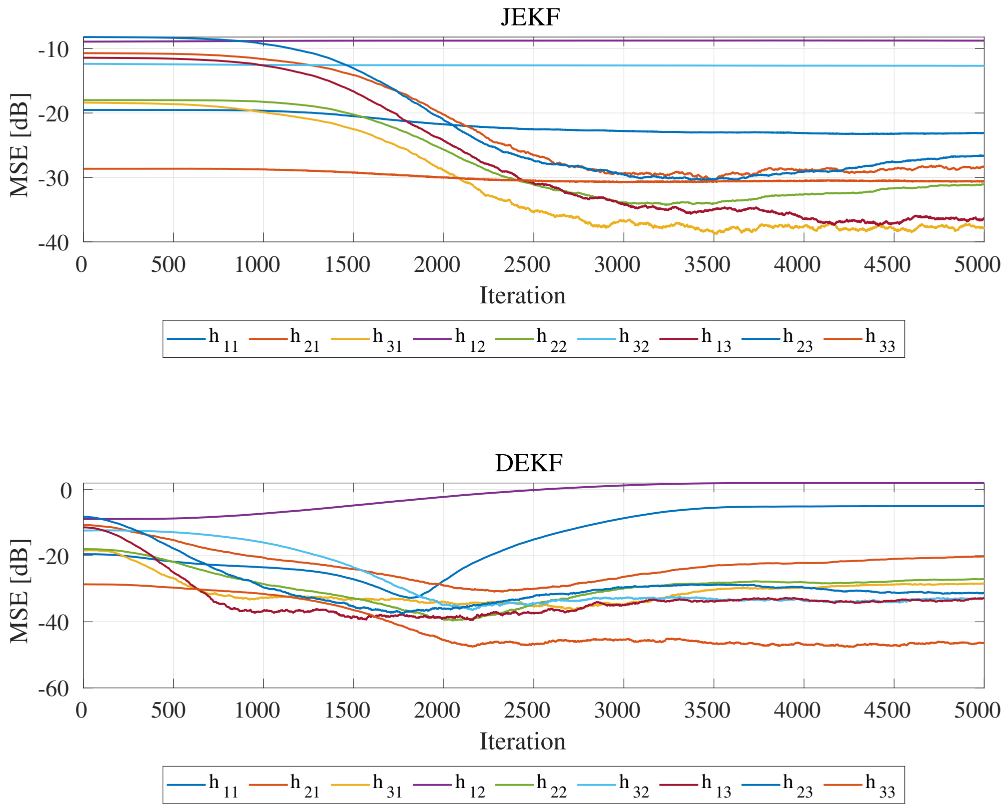

Fig. 6. Mean squared error for the estimated mixing matrix coefficients in 100 simulations of the DEKF (bottom) and JEKF (top) algorithm for N = M = 3.

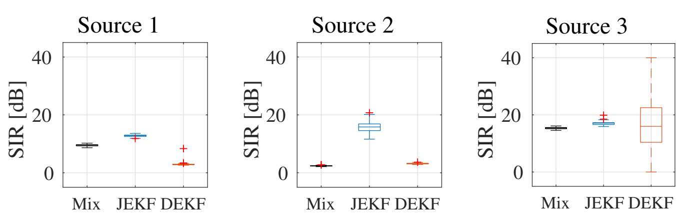

Fig. 7. SIR values for 100 simulations of the DEKF and JEKF algorithm for N = M = 3.

The JEKF and DEKF algorithms were tested in a simulation environment were their general behavior was tested by analyzing the influence of the pole values for AR(1) sources, as well as the sensitivity to the mixing matrix. The performance of the algorithms were studied and presented alongside the results for well known algorithms used in similar scenarios: SOBI and SONS.

The simulations showed that both algorithm (JEKF and DEKF) recovered mixed AR(1) sources successfully for the $N = M = 2$ scenario, for certain pole values and mixing matrix tested. However, JEKF had convergence issues depending on the initialization of the process noise covariance matrix. On the other hand, DEKF showed convergence to expected values with a performance advantage over JEKF for evaluated metrics (SIR and MER).

Fine-tuning of correlation matrices initialization and the sensitivity to the initialization of unknown parameters were found to be important for the proper functioning of JEKF and DEKF algorithms. Neither algorithm was able to perform proper parameters estimation for the mixtures involving more than two sources ($N = M = 3$).

Since the source separation is an inverse problem, from the results obtained, this ill-posed scenario may benefit of a regularization strategy, also considering the theoretical limitations of the parameter estimation approach for this model, requiring an extensive investigation and may demand an alternate solution. The absence of the results for $N >= 3$ scenarios from previous works highlights the importance of examining and discussing this limitation. A deeper analysis of the origin of these issues may lead to interesting results for perspective work.

References

[1] W. Cui, S. Guo, L. Ren, and Y. Yu, "Underdetermined blind source separation for linear instantaneous mixing system in the non-cooperative wireless communication," *Physical Communication*, vol. 45, p. 101255, 2021. doi: 10.1016/j.phycom.2020.101255

[2] A. K. Takahata, E. Z. Nadalin, R. Ferrari, L. T. Duarte, R. Suyama, R. R. Lopes, J. M. Romano, and M. Tygel, "Unsupervised processing of geophysical signals: A review of some key aspects of blind deconvolution and blind source separation," *IEEE Signal Process. Mag.*, vol. 29, no. 4, pp. 27–35, 2012. doi: 10.1109/MSP.2012.2189999

[3] M. R. Mohebbian, M. W. Alam, K. A. Wahid, and A. Dinh, "Single channel high noise level ecg deconvolution using optimized blind adaptive filtering and fixed-point convolution kernel compensation," *Biomedical Signal Processing and Control*, vol. 57, p. 101673, 2020. doi: 10.1016/j.bspc.2019.101673

[4] Q. Huang, J. Yang, Y. Xue, and Y. Zhou, "Temporally correlated source separation based on variational kalman smoother," *Digital Signal Processing*, vol. 18, no. 3, pp. 422–433, 2008. doi: 10.1016/j.dsp.2007.05.010

[5] M. Niknazar, H. Becker, B. Rivet, C. Jutten, and P. Comon, "Blind source separation of underdetermined mixtures of event-related sources," *Signal Processing*, vol. 101, pp. 52–64, 2014. doi: 10.1016/j.sigpro.2014.01.031

[6] Y. Wei and Y. Wang, "Dynamic blind source separation based on source-direction prediction," *Neurocomputing*, vol. 185, pp. 73–81, 2016. doi: 10.1016/j.neucom.2015.12.040

[7] K. T. Herring, A. V. Mueller, and D. H. Staelin, "Blind separation of noisy multivariate data using second-order statistics: Remote-sensing applications," *IEEE Trans. Geosci. Remote Sens.*, vol. 47, no. 10, pp. 3406–3415, 2009. doi: 10.1109/TGRS.2009.2022325

[8] T. Yoshioka, T. Nakatani, M. Miyoshi, and H. G. Okuno, "Blind separation and dereverberation of speech mixtures by joint optimization," *IEEE Trans. Audio, Speech, Language Process.*, vol. 19, no. 1, pp. 69–84, 2010. doi: 10.1109/TASL.2010.2045183

[9] H. Kameoka, T. Yoshioka, M. Hamamura, J. Le Roux, and K. Kashino, "Statistical model of speech signals based on composite autoregressive system with application to blind source separation," in *Latent Variable Analysis and Signal Separation: 9th International Conference, LVA/ICA 2010, St. Malo, France, September 27-30, 2010. Proceedings 9*. Springer, 2010. doi: 10.1007/978-3-642-15995-4_31 pp. 245–253.

[10] X. Gao, H. An, W. Fang, X. Huang, H. Li, and W. Zhong, "Characteristics of the transmission of autoregressive sub-patterns in financial time series," *Scientific reports*, vol. 4, no. 1, p. 6290, 2014. doi: 10.1038/srep06290

[11] A. Belouchrani, K. Abed-Meraim, J.-F. Cardoso, and E. Moulines, "A blind source separation technique using second-order statistics," *IEEE Trans. Signal Process.*, vol. 45, no. 2, pp. 434–444, 1997. doi: 10.1109/78.554307

[12] A. Cichocki, "Adaptive blind signal and image processing: Learning algorithms and applications," *John Wiley & Sons google schola*, vol. 2, pp. 1129–1159, 2002. doi: 10.1002/0470845899

[13] L. Tong, R.-W. Liu, V. C. Soon, and Y.-F. Huang, "Indeterminacy and identifiability of blind identification," *IEEE Trans. Circuits Syst.*, vol. 38, no. 5, pp. 499–509, 1991. doi: 10.1109/31.76486

[14] S. Rickard and O. Yilmaz, "On the approximate w-disjoint orthogonality of speech," in *2002 IEEE International Conference on Acoustics, Speech, and Signal Processing*, vol. 1. IEEE, 2002. doi: 10.1109/ICASSP.2002.5743771 pp. I–529.

[15] R. E. Kopp and R. J. Orford, "Linear regression applied to system identification for adaptive control systems," *Aiaa Journal*, vol. 1, no. 10, pp. 2300–2306, 1963. doi: 10.2514/3.2056

[16] R. Suyama, M. Loiola, R. Attux, and C. Junqueira, "Separação de fontes usando o filtro de kalman estendido," *XXV Simpósio Brasileiro de Telecomunicações–SBrT*, pp. 0–6, 2007. doi: 10.14209/sbrt.2007.31234

[17] L. Nelson and E. Stear, "The simultaneous on-line estimation of parameters and states in linear systems," *IEEE Trans. Autom. Control*, vol. 21, no. 1, pp. 94–98, 1976. doi: 10.1109/TAC.1976.1101148

[18] E. A. Wan and A. T. Nelson, "Dual kalman filtering methods for nonlinear prediction, smoothing and estimation," in *Advances in neural information processing systems*, 1997, pp. 793–799.

[19] ——, "Neural dual extended kalman filtering: applications in speech enhancement and monaural blind signal separation," in *Neural Networks for Signal Processing VII. Proceedings of the 1997 IEEE Signal Processing Society Workshop*. IEEE, 1997. doi: 10.1109/NNSP.1997.622428 pp. 466–475.

[20] S. Langkam and A. K. Deb, "Dual estimation approach to blind source separation," *IET Signal Processing*, vol. 11, no. 5, pp. 527–536, 2017. doi: 10.1049/iet-spr.2016.0357

[21] ——, "Convolutive blind source separation using fourier kalman filtering," in *2017 Asia Modelling Symposium (AMS)*. IEEE, 2017. doi: 10.1109/AMS.2017.27 pp. 118–124.

[22] ——, "Multiple model kalman filter approach for show-through cancellation," in *2018 IEEE 2nd International Workshop on Arabic and Derived Script Analysis and Recognition (ASAR)*. IEEE, 2018. doi: 10.1109/ASAR.2018.8480311 pp. 78–83.

[23] E. Vincent, S. Araki, and P. Bofill, "The 2008 signal separation evaluation campaign: A community-based approach to large-scale evaluation," in *International Conference on Independent Component Analysis and Signal Separation*. Springer, 2009. doi: 10.1007/978-3-642-00599-2_92 pp. 734–741.

VIII. Biography Section

Alexandre Miccheleti Lucena was born in São Bernardo do Campo, SP, Brazil, in 1993. He received the B.S. degree in science and technology from the the Federal Universisty of ABC, Santo André, SP, Brazil in 2017 with a sandwich period at the Department of Electrical Communications Engineering of the Shibaura Institute of Technology, Tokyo, Japan in 2015. He received the B.S. degree in information engineering from the Federal Universisty of ABC, the M.S. degree in information engineering from Federal University of ABC in 2021 and is currently pursuing the Ph.D. degree in information engineering at the Federal University of ABC. His research interests include digital signal processing, audio and image processing, blind source separation and machine learning.

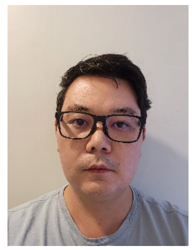

Kenji Nose Filho Kenji Nose Filho was born in Brazil in 1986. He received his B.E and M.E degrees in Electrical Engineering from São Paulo State University (UNESP), Campus of Ilha Solteira, in 2008 and 2011, respectively. During his graduation, he performed an interchange of 6 months in Universidad ORT, Montevideo, Uruguay. He received a PhD in Electrical Engineering at the State University of Campinas (UNICAMP) under the supervision of prof. João Marcos Travassos Romano and performed a PhD sandwich in GIPSA-Lab, Grenoble, France, under the supervision of prof. Christian Jutten. From September 2015 to January 2017, he was a Post-Doc at DSPCom, in the School of Electrical and Computer Engineering at UNICAMP. He is currently an assistant professor at the Federal University of ABC (UFABC), was member of the Scientific Initiation Program of the UFABC (from 2018 to 2022), vice coordinator (from 2019 to 2021) and coordinator (from 2021 to 2023) of the Undergraduate Information Engineering Course and was chair of the IEEE Signal Processing South Brazil Section Chapter (from 2019 to 2023). His research interests in signal processing are adaptive filtering, predictive deconvolution, blind source separation, machine learning, and optimization methods, with applications in reflection seismic, time-series analysis and forecasting, and image processing.

Ricardo Suyama Ricardo Suyama received his B.E., M.E., and Ph.D. degrees in Electrical Engineering from the State University of Campinas (UNICAMP) in 2001, 2003, and 2007, respectively. From 2007 to 2009, he was a Postdoctoral Researcher at DSPCom in the School of Electrical and Computer Engineering at UNICAMP. Currently, he is an Associate Professor at the Federal University of ABC (UFABC), where he served as Vice Coordinator (2011–2013) and Coordinator (2013–2015) of the Undergraduate Information Engineering program. He also served as as Vice Coordinator (2020–2024) and is current Coordinator of the Graduate Program in Information Engineering. His research interests focus on signal processing, with an emphasis on applying artificial intelligence techniques to signal and image processing.